High Frequency of Mosaicism among Patients with Neurofibromatosis Type 1 (NF1) with Microdeletions Caused by Somatic Recombination of the *JJAZ1* Gene

H. Kehrer-Sawatzki,[1] L. Kluwe,[2] C. Sandig,[1] M. Kohn,[1] K. Wimmer,[3] U. Krammer,[5] A. Peyrl,[4] D. E. Jenne,[6] I. Hansmann,[7] and V.-F. Mautner[2]

[1]Department of Human Genetics, University of Ulm, Ulm, Germany; [2]Laboratory for Tumor Biology and Development Disorders, Department of Maxillofacial Surgery, University Hospital Hamburg-Eppendorf, Hamburg, Germany; Departments of [3]Medical Biology and [4]Pediatrics, Medical University Vienna, and [5]St. Anna Children's Hospital, Vienna; [6]Department of Neuroimmunology, Max Planck Institute of Neurobiology, Martinsried, Germany; and [7]Department of Human Genetics and Medical Biology, University of Halle/Saale, Halle/Saale, Germany

Detailed analyses of 20 patients with sporadic neurofibromatosis type 1 (NF1) microdeletions revealed an unexpected high frequency of somatic mosaicism (8/20 [40%]). This proportion of mosaic deletions is much higher than previously anticipated. Of these deletions, 16 were identified by a screen of unselected patients with NF1. None of the eight patients with mosaic deletions exhibited the mental retardation and facial dysmorphism usually associated with NF1 microdeletions. Our study demonstrates the importance of a general screening for NF1 deletions, regardless of a special phenotype, because of a high estimated number of otherwise undetected mosaic NF1 microdeletions. In patients with mosaicism, the proportion of cells with the deletion was 91%–100% in peripheral leukocytes but was much lower (51%–80%) in buccal smears or peripheral skin fibroblasts. Therefore, the analysis of other tissues than blood is recommended, to exclude mosaicism with normal cells in patients with NF1 microdeletions. Furthermore, our study reveals breakpoint heterogeneity. The classic 1.4-Mb deletion was found in 13 patients. These type I deletions encompass 14 genes and have breakpoints in the NF1 low-copy repeats. However, we identified a second major type of NF1 microdeletion, which spans 1.2 Mb and affects 13 genes. This type II deletion was found in 8 (38%) of 21 patients and is mediated by recombination between the *JJAZ1* gene and its pseudogene. The *JJAZ1* gene, which is completely deleted in patients with type I NF1 microdeletions and is disrupted in deletions of type II, is highly expressed in brain structures associated with learning and memory. Thus, its haploinsufficiency might contribute to mental impairment in patients with constitutional NF1 microdeletions. Conspicuously, seven of the eight mosaic deletions are of type II, whereas only one was a classic type I deletion. Therefore, the *JJAZ1* gene is a preferred target of strand exchange during mitotic nonallelic homologous recombination. Although type I NF1 microdeletions occur by interchromosomal recombination during meiosis, our findings imply that type II deletions are mediated by intrachromosomal recombination during mitosis. Thus, NF1 microdeletions acquired during mitotic cell divisions differ from those occurring in meiosis and are caused by different mechanisms.

Introduction

Neurofibromatosis type 1 (NF1) is one of the most common autosomal dominant disorders and is caused by defects of the tumor suppressor gene, *NF1* (MIM 162200), in 17q11.2. NF1 is characterized by café-au-lait spots, neurofibromas, axillary/inguinal freckling, and Lisch nodules (Huson 1989; Marchuk and Collins

1994). Optic gliomas, bone malformations, and malignant peripheral nerve sheath tumors are also within the clinical spectrum of NF1. Furthermore, patients with NF1 often have problems in visual-spatial tasks, memory, sustained attention, coordination, language, and behavior (Gutmann et al. 1997).

Large deletions of the *NF1* gene region have been observed with a frequency of 4.4% and 4.8%, respectively, in two studies screening 500 and 84 unselected patients with NF1 (Cnossen et al. 1997; Kluwe et al. 2004). The majority of NF1 microdeletions span ~1.4 Mb, and, in ~50% of these cases, the breakpoints were mapped to low-copy repeats termed "NF1 LCRs" (López Correa et al. 1999, 2001; Dorschner et al. 2000; Jenne et al. 2000, 2001). Thus, these NF1 microdeletions belong to the group of genomic disorders that

are caused by a nonallelic homologous recombination (NAHR) between region-specific LCRs. Well-known genomic disorders caused by NAHR are Smith-Magenis syndrome (Chen et al. 1997), DiGeorge syndrome (Edelmann et al. 1999; Shaikh et al. 2000), Williams-Beuren syndrome (Peoples et al. 2000; Valero et al. 2000), Charcot-Marie-Tooth type 1A (CMT1A), and hereditary neuropathy with liability to pressure palsies (Pentao et al. 1992; Chance et al. 1994; Reiter et al. 1996). Predisposition to the deletions or duplications underlying these disorders is caused by LCRs and thus the genomic architecture of the corresponding regions (reviewed by Inoue and Lupski [2002] and Shaw and Lupski [2004]).

The NF1 LCRs, which predispose the *NF1* gene region to deletions, have a rather complicated structure. They are composed of multiple pseudogene exons of the *WI-12393* (*KIAA0563-related*) gene and segments with homology to chromosome 19. The proximal NF1 LCR encompasses 110 kb, whereas the distal NF1 LCR spans 74 kb. These LCRs are separated by ∼1.4 Mb (Dorschner et al. 2000; Jenne et al. 2000, 2001, 2003; López Correa et al. 2001). The NF1 LCRs probably originated from several duplication and transposition events during primate evolution, since they are absent in the *NF1* gene region of the mouse (Jenne et al. 2003).

In addition to the NF1 LCRs, other duplicated sequences, namely the *JJAZ1* gene and its pseudogene, are located in the *NF1* gene region. The functional *JJAZ1* gene spans 16 exons and maps 20 kb centromeric to the distal NF1 LCR (fig. 1). The *JJAZ1* pseudogene, however, encompasses only exons 1–9 and is found 41 kb distal to the proximal NF1 LCR (Jenne et al. 2003). Within 46 kb of homology between the *JJAZ1* and its pseudogene, the overall identity is 97%. The *JJAZ1* gene and its pseudogene are located in direct orientation to one another. Recently, we identified an NF1 microdeletion with breakpoints in the *JJAZ1* gene and its pseudogene (Petek et al. 2003). However, this has been the only deletion with breakpoints in the *JJAZ1* gene reported so far. The frequency of *JJAZ1*-mediated microdeletions, however, has remained unclear.

Patients with NF1 and large deletions often suffer from a more severe and atypical manifestation of disease than do the general group of patients who have NF1 with intragenic mutations. The severe and atypical phenotype is characterized by lowered mean IQ or mental retardation, facial dysmorphism, and increased risk for malignant peripheral nerve sheath tumors (Kayes et al. 1994; Wu et al. 1995; Leppig et al. 1997; Tonsgard et al. 1997; Wu et al. 1997; De Raedt et al. 2003). However, it is difficult to distinguish between patients with deletions and those without deletions solely on the basis of clinical observations. Furthermore, the majority of previous deletion studies included only preselected patients

with facial anomalies and mental retardation, whereas patients without such clinical features have usually been excluded from the deletion screening. Thus, solid evidence has been missing for the widely accepted association of NF1 microdeletion with facial anomalies and mental retardation. Additionally, it is not known whether deletion breakpoint heterogeneity influences the manifestation of symptoms in the patients.

Recently, we identified 24 *NF1* gene deletions by screening unselected patients with NF1 for polymorphic markers and by using intragenic cosmid probes in FISH (Kluwe et al. 2004; L. Kluwe, R. Siebert, S. Gesk, R. Freidrich, S. Tinschert, H. Kehrer-Sawatzki, V.-F. Mautner, unpublished data). Samples of 16 of these 24 patients were available for further analysis presented here. Additionally, we included five further deletions in our investigations. The extent of these 21 deletions was determined by use of completely sequenced and unambiguously mapped BACs, PACs, and cloned PCR products as FISH probes. Furthermore, PCR and sequence analysis was performed to identify and characterize the regions of strand exchange during the recombination underlying the deletions.

Material and Methods

Patients

The main phenotypic features of 22 patients with NF1 investigated in this study are summarized in table 1. All patients fulfill the diagnostic criteria for NF1 (Gutmann et al. 1997). Twelve patients examined here were among the 22 identified by an unselected screening of patients with NF1 performed by use of combined microsatellite marker typing and subsequent FISH (Kluwe et al. 2004). The deletions in patients 1180, 1277, 270, and 284 were identified in an updated unselected screen. Thus, in total, 16 deletions were identified on the basis of unselected screening. We investigated the deletions of six additional patients who were identified by a selective screening because of a severe phenotype (patients Z41, SR, HC, and SB) or during loss-of-heterogeneity (LOH) analysis of neurofibromas from different parts of the body (patient KCD). Patient WB is the mother of patient SB and is mildly affected, whereas the daughter has a severe phenotype. Among the 22 patients indicated in table 1, 20 patients were sporadic cases, and patients 1277 and SB were familial cases. The study protocol was approved by the institutional review board, and all participants provided informed consent.

Cell Lines

Somatic cell hybrids were generated by polyethyleneglycol-mediated fusion of thymidine-kinase–deficient mouse cell line B82 and either Epstein-Barr virus (EBV)–
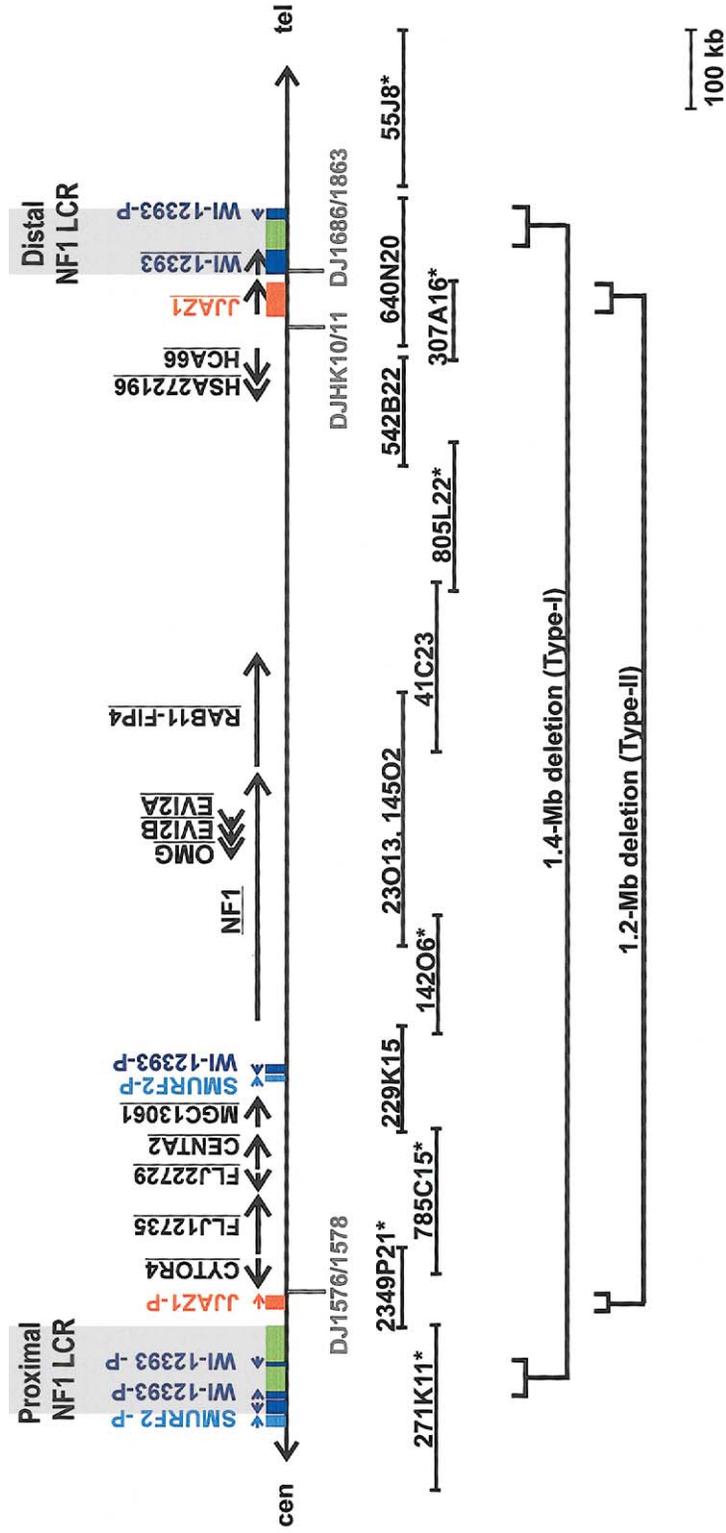
Figure 1   Map of the *NF1* gene region indicating the duplicated sequences, the genes included in type I and type II deletions, and the probes used for FISH analyses. The black horizontal arrows represent the 14 genes between and within the proximal and distal NF1 LCRs (highlighted by *gray rectangles*). The functional genes are underlined; pseudogenes are indicated with "P." The green rectangles represent the regions with homology to segments on chromosome 19. The positions of FISH probes DJ1576/1578, DJHK10/11, and DJ1686/1863 are indicated by black vertical lines. BACs and PACs that build up the contig spanning the *NF1* gene region are shown by horizontal bars. Those BACs/PACs marked by asterisks were used as FISH probes. The corresponding accession numbers are RP11-271K11 (GenBank accession number AC005562); CTD-2349P21 (GenBank accession number AC127024); RP11-785C15 (GenBank accession number AC109516); RP11-142O6 (GenBank accession number AC079915); RP11-805L22 (GenBank accession number AC007923); HCIT-307A16 (GenBank accession number AC003041); and RP11-55J8 (GenBank accession number AC015941).

Table 1

Physical Features of Patients with NF1 Microdeletions

Patient	Age (Years)	Sex	No. of Neurofibromas	Dysmorphic Facial Features[a]	Mental Retardation	Other Features	Type of Deletion	Mosaic
442[b]	25	M	>1,000	Yes	Yes[c]	High burden of subcutaneous tumors, spinal tumors	I	No
619[b]	15	F	10	Yes	Yes[d]	Astrocytoma	I	No
270	21	M	>600	Yes	Yes[c]	Plexiform neurofibroma	I	No
801[b]	38	F	>1,000	Yes	Yes	Plexiform neurofibroma	I	No
Z41	9	F	...	Yes[e]	Yes[c]	Delayed motoric development, ataxia, hamartomas of thalamus	I	No
SR	4	M	1	Yes	Yes[c]	Large ears, short stature, hyperactivity, hypogonadism, brachydactyly, camptodactyly, kyphoscoliosis	I	No
1180	15	F	...	...	Yes	MPNST	I	No
752[b]	22	F	...	?	Yes	...	I	No
450[b]	9	F	...	No	Yes[c]	...	I	No
284	40	F	...	...	Yes	...	I	No
1277	3	M	...	...	?	Family history	I	No
HC	9	M	>30	...	Yes[c]	Delayed motoric development, hamartomas of thalamus and globus pallidus	II	No
SB	35	F	>500	Yes	Yes	Kyphoscoliosis, large feet	II	No
WB[f]	65	F	>20	No	No	...	II	Yes
800[b]	49	F	>100	No	No	...	I	No
659[b]	47	F	>1,000	...	No	...	I	Yes
928[b]	35	F	12	No	No	...	II	Yes
697[b]	11	F	0	No	No	Slightly handicapped in reading and writing	II	Yes
488[b]	33	F	220	No	No	...	II	Yes
938[b]	31	F	3	No	No	MPNST	II	Yes
KCD	34	F	>100	No	No	...	II	Yes
736[b]	68	F	...	No	No	...	II	Yes

NOTE.—MPNST = malignant peripheral nerve sheath tumors.

[a] Dysmorphic features are characterized by hypertelorism, downslanting palpebral fissures, broad nose, and coarse facial appearance.

[b] These 12 patients were identified in a previous study of 500 unselected patients (Kluwe et al. 2004). The deletions in patients 1180, 1277, 270, and 284 were identified in an updated unselected screen.

[c] Mild mental retardation.

[d] Severe mental retardation.

[e] Dysmorphism in epicanthus.

[f] Mother of patient SB.

transformed lymphoblastoid cells of patient SB or skin fibroblasts of patient KCD. To confirm that the hybrids retained only one chromosome 17, FISH was performed with BAC 142O6 covering the 5′ end of the *NF1* gene and BAC 55A13 on 17q24; in addition, analyses were performed of marker D17S849, located in the deleted interval, and markers D17S1880 and D17S1841, located outside the deleted interval.

FISH Analysis

Chromosome spreads were prepared according to standard methods from whole blood samples, after culturing for 72 h in the presence of phytohemagglutinin (PHA) (Invitrogen), which mainly stimulates T lymphocytes. Therefore, we can not rule out potential selection for specific T-lymphocyte populations. After 72 h, colcemid was added and the cells were incubated for 15 min in hypotonic solution (0.075 M KCl). After centrifugation, lymphocytes were fixed with methanol and glacial acetic acid at a ratio of 3:1. The slides prepared from these suspensions were used for FISH analyses of metaphase chromosomes and interphase nuclei. Clones used as FISH probes were purchased from the BACPAC Resource Center and have been characterized elsewhere (Jenne et al. 2003). FISH was also performed with probe DJ1576/1578, which covers the region from positions 67241 to 79694 of PAC 2349P21 (GenBank accession number AC127024); probe DJHK10/11, which spans positions 4242–8373 of BAC 307A16 (GenBank accession number AC003041); and probe DJ1686/1863, which covers positions 98021–104095 of AC090616. These FISH probes were generated by PCR by use of the Expand Long Template PCR System (Roche Molecular Biochemicals) and were cloned with the TOPO TA

Cloning Kit (Invitrogen). Two-color FISH was performed by use of probes labeled with either biotin-16-dUTP or digoxygenin-11-dUTP (Roche Diagnostics). Hybridization signals were visualized with fluorescein isothiocyanate–avidin and biotinylated anti-avidin (Vector) or with anti-digoxygenin antibodies coupled to Texas Red (Dianova). Slides were counterstained with diamidinophenylindole (DAPI) and mounted with Vectashield antifade solution (Vector). Probes from the *NF1* gene region were labeled with biotin and cohybridized with the digoxygenin-labeled BAC 55A13 (GenBank accession number AC015651) from 17q24. To investigate mosaicism with normal cells, slides were hybridized with biotin-labeled BAC RP11-142O6 and digoxygenin-labeled BAC RP11-55A13. In blood lymphocytes, at least 200 interphase nuclei were evaluated, and, in buccal smears, at least 100 interphase cells were evaluated.

PCR with Somatic Cell Hybrids to Narrow the Deletion Boundaries

PCR was performed with primers P1–P4 (listed in supplementary table A1 [online-only]) to narrow the deletion boundaries by use of somatic cell hybrids that contain only the chromosome 17 with the microdeletion but not the normal chromosome 17 of the respective patient.

Oligonucleotides summarized in supplementary table A2 (online-only) were used for PCR experiments to evaluate paralogous sequence variants (PSVs) (also termed "*cis*-morphisms"), which distinguish the functional *JJAZ1* gene from its pseudogene. PCR products were sequenced by use of an ABI Prism 3100 Genetic Analyzer (Applied Biosystems).

Deletion-Junction PCR to Detect Breakpoints Located in the 2-kb Hotspot Region

To determine the frequency of type I deletions with breakpoints in the 2-kb region of preferred strand exchange described elsewhere (Jenne et al. 2001; López Correa et al. 2001), PCR was performed with primers DJ2290 (5′-TCAACCTCCCAGGCTCCCGAA-3′) and DJ2314 (5′-TTTGCACGTGTGACCTTCCACAG-3′), which detect PSVs between the proximal and the distal LCRs at their very 3′ end. Furthermore, these primers are phosphorothioated at the 3′ residue to avoid correction of the mismatches by the polymerase. As this PCR is not very robust and can lead to false-positive results, PCR products were sequenced to confirm the authenticity of a true deletion-junction fragment.

Deletion-Junction PCR to Identify Breakpoints in the JJAZ1 Sequences

To evaluate whether the breakpoints of other type II deletions map to one of the regions of strand exchange identified, PCR was performed with genomic DNA isolated from peripheral blood samples of patients with type II deletions and with the primers listed in supplementary table A3 (online-only). The primers detect PSVs at the 3′ end and are phosphorothioated at the 3′ residue. Thus, the primers discriminate between the *JJAZ1* gene and its pseudogene. PCR was performed by use of the Expand Long Template PCR System (Roche Molecular Biochemicals).

Genotyping to Determine the Mechanism Underlying the Deletions in Patients KCD and WB

Markers proximal to the *NF1* gene, D17S1873, D17S1841, D17S975, and D17S1863, as well as markers distal to the *NF1* gene, D17S1880, D17S907, D17S1833, and D17S1788, were investigated by 6FAM-labeled primers and capillary electrophoresis by use of an ABI Prism 3100 (Applied Biosystems). Markers *Rsa*I and SNP2 detect SNPs located in exon 5 of the *NF1* gene and the *RAB11-FIB4* gene, respectively. These latter markers were amplified with primers described by Eisenbarth et al. (2000).

Marker Analysis to Evaluate Mosaicism in Patient 928

Markers D17S2237 and NF1PCR were amplified by PCR with primer pairs 5′-CAAGAAAAGCTAATAT-CGGC-3′ and 5′-GGAACCTTAAGTTCACTTAG-3′ (D17S2237), and 5′-CCTCCCAAAATGCTGGGATTA-CAG-3′ and 5′-TGAGAGGCCAAGGTGAGAGAATT-GCTGGA-3′ (NF1PCR), from neurofibroma tissue sections of patient 928. Heterozygosity of these markers was detected by electrophoresis by use of an ABI Prism 3100 (Applied Biosystems).

RNA In Situ Hybridization

Pregnant C57Bl/6 mice from overnight matings were killed by cervical dislocation. The embryos and the adult mouse brain were fixed with 4% paraformaldehyde at 4°C. Serial cryosections of 10 μm were mounted on slides. RNA in situ hybridization was performed with antisense and sense riboprobes generated by in vitro transcription with T7 or Sp6 polymerase in the presence of α^{35}S-UTP (Amersham Biosciences) from linearized DNA of IMAGE cDNA clone 6513835 (GenBank accession number BQ964374), which covers exons 8–16 of the mouse *Jjaz1* mRNA. Hybridizations were performed overnight as described elsewhere (Schmid et al. 1989).

Sequence Comparisons

Sequences were aligned by use of the BLAST search facilities of the National Center for Biotechnology Information (NCBI) server and the Genetics Computer Group (GCG) software package (Wisconsin package,

version 10.2). Inverted repeats were identified by use of the program Dotter (see the Web site of the Karolinska Institutet Center for Genomics Research).

Expression Analyses of the Chimeric JJAZ1 Sequence

RNA was isolated from the hybrid cell lines SB-B9, KCD-3, and IL-39 by use of the RNeasy isolation kit (Qiagen). Reverse transcription was performed with the SuperScript transcriptase (Invitrogen). Primers located in exon 10 (5′-TACGGCTCCTATTGCCAAAC-3′) and exon 14 (5′-GCCATTCAGGATCCTTTTCA-3′) of the *JJAZ1* gene were used for RT-PCR. Products were then sequenced to confirm their authenticity.

Results

Characterization of Deletions by FISH and Deletion-Junction PCR

The extent of 21 *NF1* gene deletions was determined by FISH on metaphase chromosomes by use of seven BACs and PACs and three PCR products as probes. The position of these FISH probes in the completely sequenced contig of the *NF1* gene region is indicated in figure 1. Of the 21 deletions, 13 include the region flanked by BAC 307A16 and PAC 2349P21 (summarized in table 2). In these 13 deletion cases, BAC 271K11 shows a reduced hybridization signal. This BAC spans the proximal NF1 LCR and cohybridizes to the distal NF1 LCR. Thus, the breakpoints of these 13 deletions are located in the NF1 LCRs.

To determine whether the *WI-12393* gene is affected by the deletion, FISH was performed with probe DJ1686/1863, covering exon 1 and the promoter region of the *WI-12393* gene. No signal was obtained by this probe in all 13 cases, indicating that the corresponding sequence is deleted. Therefore, we concluded that the 13 type I NF1 microdeletions span ∼1.4 Mb and lead to hemizygosity of 14 genes, including the *WI-12393* gene.

Breakpoint-spanning PCRs were performed to evaluate how many of these type I deletions have breakpoints in the 2-kb region of preferred strand exchange described elsewhere (Jenne et al. 2001; López Correa et al. 2001). A true deletion-junction fragment was identified in 7 of 12 type I deletions for which DNA was available.

The breakpoints of the remaining eight deletions are not located in the NF1 LCRs, since BAC 307A16 and PAC 2349P21 are only partially deleted and BAC 271K11 does not decrease in signal intensity (table 2). To further narrow the breakpoints of these eight type II deletions, FISH was performed with cloned PCR products DJ1576/1578 and DJHK10/11. In all eight type II deletions, the corresponding sequences were deleted. These results imply that the breakpoints map to the *JJAZ1* gene and its pseudogene.

Identification of the Deletion Boundaries in the JJAZ1 Sequences by PCR

In two type II deletions, the breakpoints were identified by use of DNA of somatic cell hybrids that retain only the microdeleted chromosome 17 (cell lines SB-B9 and KCD-3). We also investigated hybrid cell line IL-39, which contains the chromosome 17 with the type II deletion described elsewhere (Petek et al. 2003).

The deletion boundaries were narrowed by PCR amplification of products P1–P4 from the DNA of the hybrid cell lines. The position of the primers with respect to the *JJAZ1* gene and its pseudogene is indicated in figure 2. Products P2, P3, and P4 were specifically amplified from all three hybrid cell lines (IL-39, SB-B9, and KCD-3). This indicates that the corresponding regions are not deleted. The region covered by the product P1, however, turned out to be deleted in all three hybrids.

PSVs (paralogous sequence variants), which distinguish the *JJAZ1* gene from the pseudogene, were evaluated to identify the regions of strand exchange. These PSVs were discriminated from polymorphisms by the comparison to published BAC sequences, by sequence analysis of PCR products amplified from three somatic cell hybrids that contain a nondeleted chromosome 17 and by sequence analysis of PCR products amplified from those three hybrids with the recombinant *JJAZ1* gene.

In cell line KCD-3, the transition of proximal to distal PSVs, which indicates the region of strand exchange, was identified in intron 4 between nucleotides 29666 and 29776 (BAC 640N20 [GenBank accession number AC090616]) (fig. 3). The deletion breakpoint in hybrid IL-39 was mapped in intron 5 between nucleotides 51928 and 51976. The crossover region of the deletion in patient SB was identified in intron 8 between nucleotides 61762 and 62015. This latter region includes a partial L1 and an *Alu* element. In contrast, the regions of strand exchange in introns 4 and 5 occurred in single-copy segments.

Deletion-Junction PCR to Amplify across the Regions of Strand Exchange in the JJAZ1 Sequences

To evaluate whether the breakpoints of the other six type II deletions map to one of the identified regions of strand exchange, deletion-junction PCRs were performed. These PCRs amplify the breakpoint regions identified in introns 4, 5, or 8, respectively. Since the breakpoint regions in introns 5 and 8 are separated by only 10 kb, we also investigated the segment between both regions by deletion-junction PCR. None of the remaining six type II deletions was positive for one of these PCRs.

Table 2

Characterization of the Deletion Breakpoint Boundaries by FISH and Breakpoint-Spanning PCR Analysis

| | RESULTS OF FISH ANALYSIS WITH BACs/PACs | | | | | | | DELETION-JUNCTION PCR | % OF CELLS WITH DELETION IN | |
| | | | | | | | | | Peripheral Blood | Other Tissue |
PATIENT	271K11	2349P21	785C15	142O6	805L22	307A16	55J8			
442	P	D	D	D	D	D	N	−	100	ND
619	P	D	D	D	D	D	N	−	100	ND
270	P	D	D	D	D	D	N	+	100	ND
801	P	D	D	D	D	D	N	−	100	ND
Z41	P	D	D	D	D	D	N	ND	100	ND
SR	P	D	D	D	D	D	N	+	100	ND
1180	P	D	D	D	D	D	N	−	100	ND
752	P	D	D	D	D	D	N	+	100	ND
450	P	D	D	D	D	D	N	+	100	ND
284	P	D	D	D	D	D	N	+	100	100[a]
1277	P	D	D	D	D	D	N	+	100	100[a]
800	P	D	D	D	D	D	N	+	100	ND
659	P	D	D	D	D	D	N	−	96	52[a]
SB	N	P	D	D	D	P	N	+	100	ND
WB[b]	N	P	D	D	D	P	N	+	94	ND
HC	N	P	D	D	D	P	N	−	100	ND
928	N	P	D	D	D	P	N	−	100	55[a]; 80[c]
697	N	P	D	D	D	P	N	−	97	59[a]
488	N	P	D	D	D	P	N	−	98	56[a]
938	N	P	D	D	D	P	N	−	91	80[a]
KCD	N	P	D	D	D	P	N	+	92	51[d]
736	N	P	D	D	D	P	N	−	94	59[a]

NOTE.—The plus sign (+) indicates positive deletion-junction PCR, as determined by sequence analysis; the negative sign (−) indicates negative deletion-junction PCR, as determined by sequence analysis. D = deleted; N = not deleted; P = partially deleted; ND = not determined.

[a] Buccal smears.
[b] Mother of patient SB.
[c] Neurofibroma.
[d] Skin fibroblasts cultured from a skin biopsy.

Sequence Analysis of the Breakpoint Regions

The breakpoint regions in introns 4, 5, and 8 of the *JJAZ1* gene were screened for the presence of recombinogenic motifs (summarized by Abeysinghe et al. [2003]). Only in the 253-bp segment of strand exchange in intron 8 was such a motif found—namely, a translin binding site.

To identify structural features that might have mediated double-strand breaks during recombination, the *JJAZ1* sequences were scanned for inverted repeats. These analyses indicated that the region of strand exchange in intron 5 is flanked by an inverted repeat of 127 bp, with 88% identity. Also, the region of strand exchange in intron 8 is flanked by a small inverted repeat of 75 bp, with 74% identity. However, inverted repeats are not present in the crossover region of intron 4.

The average GC content of the *JJAZ1* gene and its pseudogene is 41%. The GC content of the regions of strand exchange in introns 4, 5, or 8 is not above this average.

Expression Analysis of the Recombinant JJAZ1 *Fusion Gene*

The recombination between the *JJAZ1* pseudogene and the functional gene leads to a chimeric gene with the pseudogene at the 5′ end and part of the functional gene at the 3′ end. RT-PCR and sequencing of the respective products indicated that the recombinant *JJAZ1* gene is expressed in hybrid cell lines SB-B9, KCD-3, and IL-39. Correspondingly, the fusion transcript of the *JJAZ1* pseudogene and the functional *JJAZ1* gene is not prone to nonsense-mediated mRNA decay. It is not very likely that the chimeric mRNA is efficiently translated, as stop codons are found in exon 2 of the pseudogene, truncating the ORF prematurely. Additionally, internal methionine codons located in exons 3 and 4 are not embedded in a KOZAK sequence.

Mosaicism in Patients with NF1 Microdeletions

Analysis of peripheral blood, buccal mucosa, skin fibroblasts, or neurofibroma tissue revealed mosaicism for
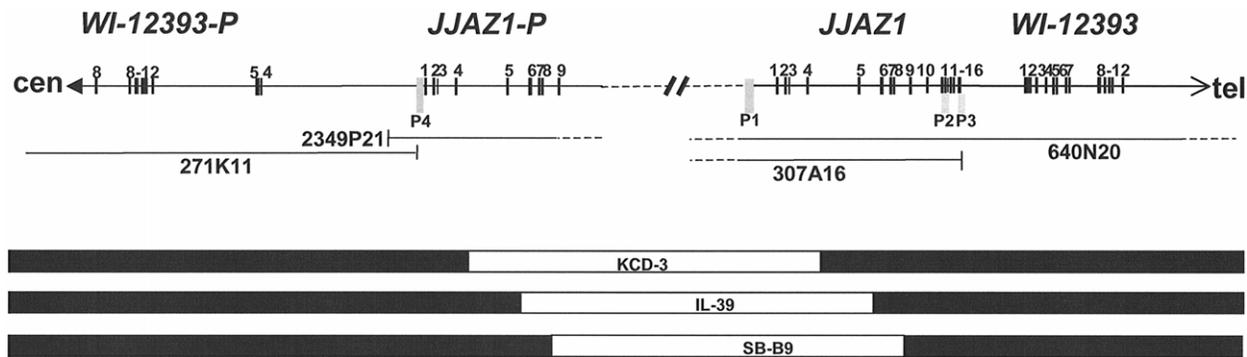
Figure 2   Position of the deletion breakpoints in patients SB and KCD (investigated in this study) and in patient IL (described elsewhere) (Petek et al. 2003). The precise breakpoints in the *JJAZ1* gene and its pseudogene (*JJAZ-P*) were identified by use of somatic cell hybrids that contain only the deleted chromosome 17 (cell lines KCD-3, IL-39, and SB-B9). Black bars indicate the nondeleted regions; white bars represent the deletion intervals. Exon numbers are given above, and the regions covered by PCR products P1–P4 are marked by gray rectangles.

microdeletions in eight cases (table 2 and supplementary table A4 [online-only]). Six of the mosaic microdeletions were found among the 24 patients with deletions who were identified by an unselected screen (Kluwe et al. 2004; L. Kluwe, R. Siebert, S. Gesk, R. Freidrich, S. Tinschert, H. Kehrer-Sawatzki, V.-F. Mautner, unpublished data). This gives a frequency of mosaicism of at least 26% among the 23 patients with no family history for NF1 (6/23). In seven of the eight mosaic deletions, the breakpoints were assigned to the *JJAZ1* gene (table 2). A very peculiar form of somatic mosaicism was observed in patient 928. In peripheral blood lymphocytes, the deletion was detected by FISH in 100% of the cells. However, in sections of a dermal neurofibroma, 20% of the nuclei, likely nontumor cells, had two FISH signals of BAC 142O6. Mosaicism was further confirmed in this patient by heterozygosity of two markers located in the *NF1* gene in DNA extracted from this tumor. Furthermore, normal cells were detected by FISH in 45% of buccal cells.

These findings prompted us to search for mosaicism in families with a microdeletion in the offspring. Patient WB is mildly affected, whereas her daughter, SB, has a severe manifestation and an NF1 microdeletion. Attentive analysis of blood lymphocytes of patient WB revealed mosaicism for a type II deletion she passed on to her daughter, SB (table 2).

Mechanism Underlying the Deletion in Patients KCD and WB

The recombination mechanism underlying the mosaic type II deletions identified in patients KCD and WB was evaluated by marker analysis (fig. 4). The haplotypes of patient KCD were identified by use of somatic cell hybrids that contain only one chromosome 17. Hybrid-line KCD-101 retains the normal chromosome 17, whereas hybrid

KCD-25 contains the normal chromosomes 17 prior to the deletion. Hybrid KCD-3, however, contains the chromosome 17 with the microdeletion. In patient SB, the phase of markers was determined with hybrids that contained either the normal chromosome 17 (SB-B10) or the microdeleted chromosome 17 (SB-B9). Marker analysis in the mother, patient WB, was performed with DNA of an EBV-transformed lymphoblastoid cell line, with 30% normal cells and 70% microdeleted cells. According to parsimony considerations, the deletion in patient KCD, as well as that in patient WB, occurred by intrachromosomal recombination during mitosis.

Expression Analysis of the JJAZ1 *Gene by RNA In Situ Hybridization*

In view of the paucity of knowledge about the function of the *JJAZ1* gene, we performed RNA in situ hybridization by use of mouse tissue sections to identify the sites of highest *Jjaz1* expression (fig. 5A–5H). At an early developmental stage (embryonal day [ED] 9,5), *Jjaz1* is ubiquitously expressed in the embryo proper and in the labyrinth of the placenta (fig. 5F). During later development, at ED14,5, prominent *Jjaz1* expression is noticed in the liver, the lung, and the kidneys, as well as in the developing neocortex in subventricular zones (fig. 5H). In the adult mouse brain, *Jjaz1* is highly expressed in the hippocampus, the pyriform cortex, the habenula, the granular cell layer of the cerebellum, and the surrounding Purkinje cells (fig. 5B and 5D).

Discussion

Two Types of NF1 Microdeletions

Previous studies showed that, in ~50% of NF1 microdeletions, the breakpoints are located in the NF1 LCRs (López Correa et al. 1999, 2001; Dorschner et al.
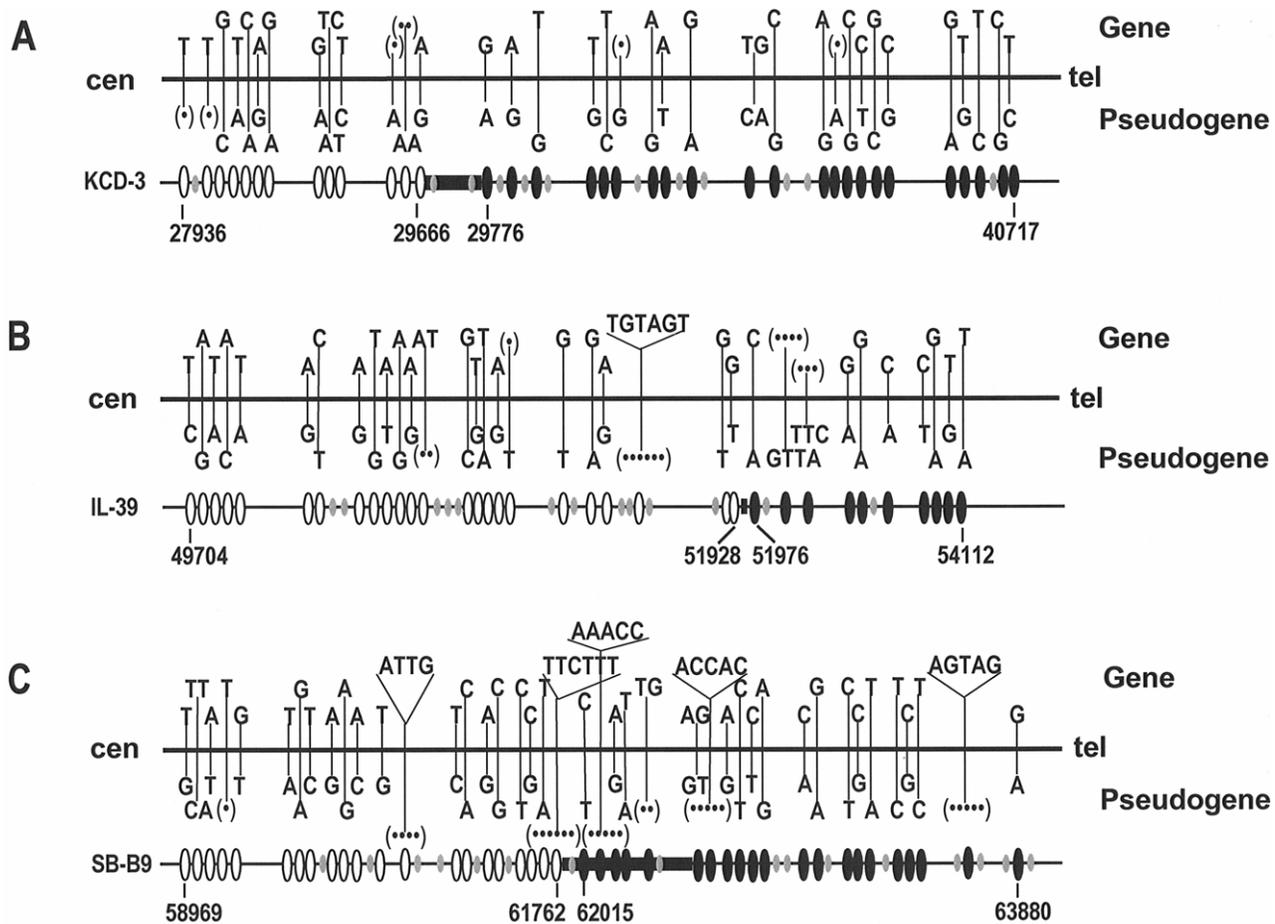
Figure 3 Areas of strand exchange in the recombinant *JJAZ1* sequences of patients KCD (*A*), SB (*B*), and IL (*C*), as determined by use of somatic cell hybrids that contain only the chromosome 17 with the deletion found in the respective patient. The regions of strand exchange, marked by black rectangles, were identified by the analysis of nucleotide differences between the *JJAZ1* gene located distal and its pseudogene located proximal to the *NF1* gene. The nucleotides typical for the *JJAZ1* gene are given above the respective lines, and those characteristic for the pseudogene are given below. White ovals indicate that the sequence amplified from the hybrid cell line corresponds to the *JJAZ1* pseudogene sequence; black ovals denote matches to the functional *JJAZ1* gene. Noninformative polymorphisms (sequence differences among individuals) are represented as gray ovals. The numbers indicate the position of the respective PSV according to AC090616 (BAC 640N20).

2000; Jenne et al. 2000, 2001). In our sample, 13 (62%) of 21 deletions have breakpoints in the NF1 LCRs (table 2). FISH analyses indicated that the *WI-12393* (*KIAA0563-related*) gene is included in the deleted region in the 13 type I deletions. Thus, all of the 13 type I deletions span 1.4 Mb and encompass 14 functional genes.

Our study further revealed a second major type of NF1 microdeletion. In 8 (38%) of the 21 deletions, the breakpoints occurred in the *JJAZ1* gene and its pseudogene (table 2). These type II deletions span 1.2 Mb and encompass only 13 genes, since the functional *WI-12393* gene is retained (fig. 1). It is interesting that seven (88%) of eight type II deletions are mosaic deletions and are found in female patients.

Somatic Mosaicism in NF1 Microdeletions

Among the 24 deletions identified in a previous (Kluwe et al. 2004) and updated screening of unselected patients with NF1 (L. Kluwe et al., unpublished data), 6 were found to be mosaic deletions in this study, giving a minimum frequency of mosaicism of 26% (6/23 cases without family history). Until now, mosaicism of NF1 microdeletions has been observed in only a few cases (summarized in Petek et al. 2003). Rasmussen et al. (1998) detected two mosaic NF1 microdeletions by LOH analysis and suggested that mosaicism might be more frequent than was previously assumed. The most obvious reason for the underestimation of mosaicism is that deletion screening is mostly restricted to patients

A

	KCD Blood		Hybrid KCD-101	Hybrid KCD-25	Hybrid KCD-3
D17S1873	140	140	140	140	140
D17S1841	270	272	272	270	270
D17S975	254	258	258	254	254
D17S1863	256	254	254	256	256
RsaI-Ex.5	1	2	2	1	—
SNP2	1	2	2	1	—
D17S1880	181	183	183	181	181
D17S907	299	311	311	299	299
D17S1833	154	156	156	154	154
D17S1788	166	155	155	166	166

B

I/1

II/1 II/2

	WB EBV		Hybrid SB-10	Hybrid SB-9	II/2	
D17S1873	125	134	130	134	125	130
D17S1841	272	278	265	278	272	265
D17S975	259	259	263	259	259	263
D17S1863	256	254	256	254	256	256
D17S1849	208	208	210	—	208	210
SNP2	1	1	1	—	1	1
D17S1880	182	182	174	182	182	174
D17S907	319	323	323	323	319	323
D17S1833	154	154	154	154	154	154
D17S1788	156	156	160	156	156	160

Figure 4 Genotype analysis to determine that the type II deletion in patients KCD (*A*) and WB (*B*) occurred by intrachromosomal recombination. Eight polymorphic markers that flank the *NF1* gene region and are located outside of the deletion interval were investigated. In addition, two markers within the deletion interval (*Rsa*I and SNP2) were analyzed. *A*, The haplotypes were determined by the analysis of hybrid cell line KCD-3 with the microdeleted chromosome 17, hybrid cell line KCD-25 with chromosome 17 prior to the deletion, and hybrid cell line KCD-101, which retains the unaffected chromosome 17. *B*, Patient WB shows mosaicism for the type II deletion. The phase of markers was determined in her daughter, SB, by use of hybrid cell line SB-10 with the normal chromosome 17 and cell line SB-B9 with the microdeleted chromosome 17. The gray rectangles highlight the haplotype of the chromosome with the microdeletion.

with mental retardation and facial dysmorphism. However, none of the patients with mosaic deletions in our study had these features. These deletions would not have been identified by restricted screens. Our recent screening included all patients, even those with no clinical indication of an NF1 microdeletion, which enabled the identification of patients with mosaicism.

Another reason for the underestimation of mosaicism in NF1 microdeletions might be that the number of cells with the deletion is extremely high in peripheral blood, the tissue most commonly used for deletion analysis. Our results demonstrate that, in comparison to peripheral blood, normal cells are far more frequent in other peripheral tissues, like buccal smears or skin fibroblasts. An extreme case of mosaicism is patient 928. The deletion was detected by FISH in 100% of the lymphocytes. However, normal cells were identified in 20% of neurofibroma cells and in 45% of buccal cells. These findings suggest that hematopoietic stem cells with an NF1 microdeletion have a significant growth advantage, compared with normal cells.

Positional Preference of NAHR in NF1 Microdeletions

Specific sequences or genomic architectural features predispose to NAHR between duplicated sequences (for review, see Inoue and Lupski 2002; Stankiewicz and Lupski 2002; Lupski 2003; Shaw and Lupski 2004). In some of the LCR-mediated genomic disorders, hotspots of positional preference for strand exchange during recombination were identified. For instance, a 557-bp region in the 24-kb CMT1A-REPs in 17p11.2 is involved in ~78% of crossovers in CMT1A (Reiter et al. 1998). In Williams-Beuren syndrome, >27% of deletion breakpoints occurred in a 12-kb region of the much-larger LCRs in 7q11.23 (Bayes et al. 2003). Recently, Bi et al. (2003) observed that, despite ~170 kb of high homology, 50% of the recombinant junctions of the 4-Mb deletions in Smith-Magenis syndrome map to a 12-kb region. As predicted by reciprocal recombination, junction fragments in patients with dup(17)(p11,2p11.2) were also mapped to this hotspot region.

Positional preference for recombination was also found in NF1 LCR–mediated microdeletions in a segment of 2 kb (Jenne et al. 2001; López Correa et al. 2001). This hotspot is confirmed in our study, since 58% of the type I deletions had breakpoints in this interval. Our results further indicate that, in addition to the NF1 LCRs, the *JJAZ1* gene is also a preferred region of NAHR leading to NF1 microdeletions. In three *JJAZ1*-mediated type II deletions, the regions of strand exchange were identified in introns 4, 5, and 8 of the *JJAZ1* gene, respectively (figs. 2 and 3). The breakpoint regions in introns 5 and 8 are separated by only 10 kb.

Structural Motifs or Sequence Elements That Stimulate Strand Exchange between the JJAZ1 *Sequences*

DNA motifs—like χ elements, minisatellite core sequences, and several other motifs summarized by Abeysinghe et al. (2003)—are well known to promote recombination. We screened the breakpoint regions in *JJAZ1*
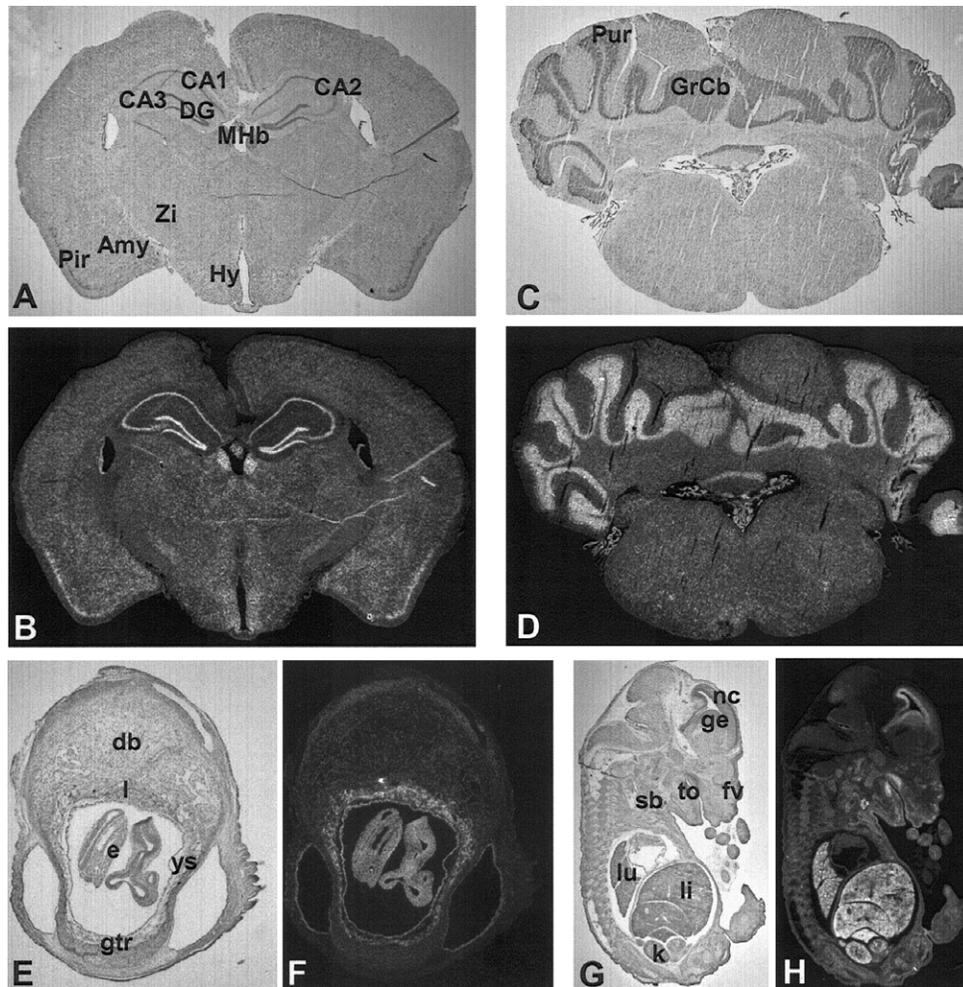
Figure 5   Expression pattern of the mouse *Jjaz1* mRNA in coronal sections of the adult mouse brain (*A–D*), horizontal sections of ED9,5 (*E* and *F*), and sagittal sections of ED14,5 embryos (*G* and *H*). Bright-field images are stained with Giemsa (*A, C, E,* and *G*). The corresponding dark-field images (*B, D, F,* and *H*) indicate as white areas the regions of highest *Jjaz1* expression. Amy = amygdala; CA1–3 = regions of the hippocampus; db = decidua basalis; DG = dentate gyrus; e = embryo; fv = primordium of follicle of vibrissae; ge = ganglionic eminence; gtr = trophoblast giant cell; GrCb = granular cell layer of cerebellum; k = kidney; l = labyrinth; li = liver; lu = lung; MHb = medial habenular nucleus; nc = neocortex; Hy = hypothalamus; sb = submandibular gland; to = upper and lower molar tooth; Pur = Purkinje cells; Pir = piriform cortex; ys = yolk sac; and Zi = zona incerta.

introns 4, 5, and 8 for such motifs. Only in the region of strand exchange in intron 8 was a recombinogenic motif identified—namely, a translin binding site. Translin is known to bind to single-stranded ends of staggered breaks during DNA repair (Sengupta and Rao 2002). Translin binding sites were found to be significantly overrepresented near both translocation and deletion breakpoints (Abeysinghe et al. 2003). It remains to be experimentally proven whether strand exchange is indeed promoted by this mechanism.

Among the structural genomic features that are able to stimulate recombination are inverted repeats. They cause double-strand breaks by forming hairpin-like structures (Gordenin and Resnick 1998), thus initiating nonhomologous recombination. The breakpoint region in intron 5 is flanked by an inverted repeat of 127 bp. Also, the region of strand exchange in intron 8 is flanked by an inverted repeat of 75 bp. Hypothetically, these inverted repeats form hairpin loops that cause double-strand breaks during the recombination process. It has been suggested that a certain length of perfect identity of 300–500 bp is required for effective NAHR (Reiter et al. 1998; López Correa et al. 2001; Bi et al. 2003). To investigate a possible correlation of strand exchange and regions of perfect identity, we compared the proximal and distal *JJAZ1* sequences by pairwise alignment. In the regions of strand exchange in introns 4 and 5, no segments of perfect identity larger than 100 bp were

found. In the region of crossover in intron 8, however, a segment of 252 bp, with 100% identity, was detected.

In summary, several sequence motifs or structural features were identified that might facilitate strand exchange in the *JJAZ1* sequences. However, none of the identified crossover regions reveals conspicuous features like a high density of recombinogenic motifs or inverted repeats of 2 kb. Such features have been identified in the breakpoint regions of SMS-REP–mediated deletions and duplications (Bi et al. 2003). Deletion-junction PCRs that amplify across the breakpoints in *JJAZ1* introns 4, 5, or 8 were negative in the other six patients with type II deletions. Thus, a highly restricted positional preference of NAHR in the *JJAZ1* gene is not very likely. The multitude of polymorphisms, however, found in introns 4, 5, and 8 indicates that allelic nonaberrant recombination occurs quite commonly in the respective regions (fig. 3).

Positional Preference for Somatic Nonallelic Recombination in the JJAZ1 Gene

Conspicuously, the breakpoints of seven of the eight mosaic deletions are located in the *JJAZ1* gene and its pseudogene. Thus, the *JJAZ1* gene is a preferred target of strand exchange during somatic NAHR, leading to NF1 microdeletions. Although the NF1 LCRs are also involved in somatic recombination, as indicated by mosaicism of a type I deletion in patient 659, mitotic NAHR seems to be much more frequent in the *JJAZ1* gene and its pseudogene. The reason for this preference is unknown.

The function of the *JJAZ1* gene, which is completely deleted in patients with type I NF1 microdeletions and is disrupted in deletions of type II, is not well characterized. It encodes an 803-aa protein with a zinc-finger domain and has extensive homology to the *Drosophila* protein Suppressor of zeste (Suz12), which belongs to the Polycomb group of proteins. It is interesting that *JJAZ1* is highly expressed in the cerebellum, the Purkinje cells, the pyriform cortex, and the pyramidal cells of the hippocampus in the mouse brain (fig. 5). Neurons in these structures are characterized by the highest synaptic activity in the whole brain (Malenka and Nicoll 1999; Bliss et al. 2000). The hippocampus is an essential component in cognitive function and learning. The cells of the pyriform cortex are linked to the formation of the amygdala, which has been associated with a range of cognitive functions, including emotion, learning, memory, attention, and perception (Gallagher and Chiba 1996). Therefore, the *JJAZ1* gene is a candidate gene whose haploinsufficiency contributes to mental impairment in patients with constitutional NF1 microdeletions.

The *JJAZ1* gene has recently been shown to be disrupted by the somatically acquired translocation t(7;17) in endometrial stromal tumors. This translocation leads to the fusion of the *JJAZ1* gene in 17q11.2 with the *JAZF1* gene on chromosome 7, which also encodes for a protein with a zinc-finger domain (Koontz et al. 2001). The breakpoint of t(7;17) was mapped to intron 1 of the *JJAZ1* gene by Koontz et al. (2001). Although the breakpoints in introns 4, 5, and 8 identified in NF1 microdeletions in the present study are located more distally, these data underscore that the *JJAZ1* gene is a preferred target for somatic aberrant recombination.

Recombination Mechanism Underlying Type I and Type II Deletions

The type II deletions identified in patients KCD and WB were mediated by intrachromosomal recombination (fig. 4). Additionally, the *JJAZ1*-mediated deletion in patient IL arose by intrachromosomal NAHR (Petek et al. 2003). In contrast, the majority of type I deletions are generated by interchromosomal recombination between the NF1 LCRs during germ-cell development (López Correa et al. 2000). Thus, the underlying mechanism differs between type I and type II NF1 microdeletions.

Genotype/Phenotype Correlations in Patients with NF1 Microdeletions

Our study clearly indicates breakpoint heterogeneity among patients with NF1 microdeletions. The 1.4-Mb–spanning type I deletion includes the functional *WI-12393* gene, which is retained in the smaller type II deletion of 1.2 Mb. Mental retardation in patient SB, who has a type II deletion, shows that *WI-12393* hemizygosity does not play a key role in this special phenotype. Nevertheless, the clinical spectrum of patients with type I and type II deletions may differ. Further investigations with larger numbers of clinically well-characterized patients with NF1 microdeletions are recommended to address this issue. Furthermore, somatic mosaicism is a hitherto-unappreciated factor that influences genotype/phenotype correlations. None of the patients with mosaicism for an NF1 microdeletion investigated in our study is mentally retarded or has facial dysmorphism. Normal facial configuration and intelligence was also found in patient 800, who had a type I deletion in 100% of the lymphocytes. We also suspect mosaicism in this exceptional patient, but somatic tissues other than blood were not available for further analyses.

In our study, a total of nine patients with deletions did not exhibit the mental retardation and facial dysmorphism that was believed to be strictly associated with NF1 microdeletions. These patients would not have been identified if the deletion screen had been restricted to patients with such phenotypes, as was the case in most previous deletion studies and is still the case in some laboratories. Our results suggest a general screening for

NF1 microdeletions, regardless of the presence of special phenotypes.

Acknowledgments

Electronic-Database Information

Accession numbers and URLs for data presented herein are as follows:

BACPAC Resource Center Home Page, http://bacpac.chori .org/

GenBank, http://www.ncbi.nlm.nih.gov/Genbank/ (for PAC 2349P21 [accession number AC127024], BAC 307A16 [accession number AC003041], BAC 55A13 [accession number AC015651], cDNA clone 6513835 [accession number BQ964374], BAC 640N20 [accession number AC090616], RP11-271K11 [accession number AC005562], CTD-2349P21 [accession number AC127024], RP11-785C15 [accession number AC109516], RP11-142O6 [accession number AC079915], RP11-805L22 [accession number AC007923], HCIT-307A16 [accession number AC003041], and RP11-55J8 [accession number AC015941])

Karolinska Institutet Center for Genomics Research, http://www .cgr.ki.se/cgr/groups/sonnhammer/Dotter.html (for Dotter program)

National Center for Biotechnology Information, http://www .ncbi.nlm.nih.gov/

Online Mendelian Inheritance in Man (OMIM), http://www .ncbi.nlm.nih.gov/Omim/ (for *NF1*)

RepeatMasker, http://www.repeatmasker.org/

References

Abeysinghe SS, Chuzhanova N, Krawczak M, Ball EV, Cooper DN (2003) Translocation and gross deletion breakpoints in human inherited disease and cancer I: nucleotide composition and recombination-associated motifs. Hum Mutat 22: 229–244

Bayes M, Magano LF, Rivera N, Flores R, Perez Jurado LA (2003) Mutational mechanisms of Williams-Beuren syndrome deletions. Am J Hum Genet 73:131–151

Bi W, Park SS, Shaw CJ, Withers MA, Patel PI, Lupski JR (2003) Reciprocal crossovers and a positional preference for strand exchange in recombination events resulting in deletion or duplication of chromosome 17p11.2. Am J Hum Genet 73: 1302–1315

Bliss T, Errington M, Fransen E, Godfraind JM, Kauer JA, Kooy RF, Maness PF, Furley AJ (2000) Long-term potentiation in mice lacking the neural cell adhesion molecule L1. Curr Biol 10:1607–1610

Chance PF, Abbas N, Lensch MW, Pentao L, Roa BB, Patel PI, Lupski JR (1994) Two autosomal dominant neuropathies result from reciprocal DNA duplication/deletion of a region on chromosome 17. Hum Mol Genet 3:223–228

Chen KS, Manian P, Koeuth T, Potocki L, Zhao Q, Chinault AC, Lee CC, Lupski JR (1997) Homologous recombination of a flanking repeat gene cluster is a mechanism for a common contiguous gene deletion syndrome. Nat Genet 17:154–163

Cnossen MH, van der Est MN, Breuning MH, van Asperen CJ, Breslau-Siderius EJ, van der Ploeg AT, de Goede-Bolder A, van den Ouweland AM, Halley DJ, Niermeijer MF (1997) Deletions spanning the neurofibromatosis type 1 gene: implications for genotype-phenotype correlations in neurofibromatosis type 1? Hum Mutat 9:458–464

De Raedt T, Brems H, Wolkenstein P, Vidaud D, Pilotti S, Perrone F, Mautner V, Frahm S, Sciot R, Legius E (2003) Elevated risk for MPNST in NF1 microdeletion patients. Am J Hum Genet 72:1288–1292

Dorschner MO, Sybert VP, Weaver M, Pletcher BA, Stephens K (2000) NF1 microdeletion breakpoints are clustered at flanking repetitive sequences. Hum Mol Genet 9:35–46

Edelmann L, Pandita RK, Morrow BE (1999) Low-copy repeats mediate the common 3-Mb deletion in patients with velo-cardio-facial syndrome. Am J Hum Genet 64:1076–1086

Eisenbarth I, Vogel G, Krone W, Vogel W, Assum G (2000) An isochore transition in the *NF1* gene region coincides with a switch in the extent of linkage disequilibrium. Am J Hum Genet 67:873–880

Gallagher M, Chiba A (1996) The amygdala and emotion. Curr Opin Neurobiol 6: 221–227

Gordenin DA, Resnick MA (1998) Yeast ARMs (DNA at-risk motifs) can reveal sources of genome instability. Mutat Res 400:45–58

Gutmann D, Aylsworth A, Carey J, Korf B, Marks J, Pyeritz R, Rubenstein A, Viskochil D (1997) The diagnostic evaluation and multidisciplinary management of neurofibromatosis 1 and neurofibromatosis 2. JAMA 278:51–57

Huson SM (1989) Recent developments in the diagnosis and management of neurofibromatosis. Arch Dis Child 64:745–749

Inoue K, Lupski JR (2002) Molecular mechanisms for genomic disorders. Annu Rev Genomics Hum Genet 3:199–242

Jenne DE, Tinschert S, Dorschner MO, Hameister H, Stephens K, Kehrer-Sawatzki H (2003) Complete physical map and gene content of the human NF1 tumor suppressor region in human and mouse. Genes Chromosomes Cancer 37:111–120

Jenne DE, Tinschert S, Stegmann E, Reimann H, Nürnberg P, Horn D, Naumann I, Buske A, Thiel G (2000) A common set of at least 11 functional genes is lost in the majority of NF1 patients with gross deletions. Genomics 66:93–97

Jenne DE, Tinschert S, Reimann H, Lasinger W, Thiel G, Hameister H, Kehrer-Sawatzki H (2001) Molecular characterization and gene content of breakpoint boundaries in patients with neurofibromatosis type 1 with 17q11.2 microdeletions. Am J Hum Genet 69:516–527

Kayes LM, Burke W, Riccardi VM, Benett R, Ehrlich P, Rubinstein A, Stephens K (1994) Deletions spanning the neurofibromatosis I gene: identification and phenotype of five patients. Am J Hum Genet 54:424–436

Koontz JI, Soreng AL, Nucci M, Kuo FC, Pauwels P, van Den Berghe H, Cin PD, Fletcher JA, Sklar J (2001) Frequent fusion of the *JAZF1* and *JJAZ1* genes in endometrial stromal tumors. Proc Natl Acad Sci USA 98:6348–6353

Kluwe L, Siebert R, Gesk S, Freidrich RE, Tinschert S, Kehrer-Sawatzki H, Mautner V-F (2004) Screening of 500 unselected neurofibromatosis 1 patients for deletions of the *NF1* gene. Hum Mutat 23:111–116

Leppig KA, Kaplan P, Viskochil D, Weaver M, Ortenberg J, Stephens K (1997) Familial neurofibromatosis 1 microdeletions: cosegregation with distinct facial phenotype and early onset of cutaneous neurofibromata. Am J Med Genet 73:197–204

López Correa C, Brems H, Lazaro C, Estivill X, Clementi M, Mason S, Rutkowski JL, Marynen P, Legius E (1999) Molecular studies in 20 submicroscopic neurofibromatosis type 1 gene deletions. Hum Mutat 14:387–393

López Correa C, Brems H, Lazaro C, Marynen P, Legius E (2000) Unequal meiotic crossover: a frequent cause of NF1 microdeletions. Am J Hum Genet 66:1969–1974

López Correa C, Dorschner M, Brems H, Lazaro C, Clementi M, Upadhyaya M, Dooijes D, Moog U, Kehrer-Sawatzki H, Rutkowski JL, Fryns JP, Marynen P, Stephens K, Legius E (2001) Recombination hotspot in NF1 microdeletion patients. Hum Mol Genet 10:1387–1392

Lupski JR (2003) 2002 Curt Stern Award Address. Genomic disorders recombination-based disease resulting from genomic architecture. Am J Hum Genet 72:246–252

Malenka RC, Nicoll RA (1999) Long-term potentiation: a decade of progress? Science 285:1870–1874

Marchuk DA, Collins FS (1994) Molecular genetics of neurofibromatosis 1. In: Huson SM, Hughes RAC (eds) The neurofibromatoses: a pathogenetic and clinical overview. Chapman and Hall, London, pp 23–49

Pentao L, Wise CA, Chinault AC, Patel PI, Lupski JR (1992) Charcot-Marie-Tooth type 1A duplication appears to arise from recombination at repeat sequences flanking the 1.5 Mb monomer unit. Nat Genet 2:292–300

Peoples R, Franke Y, Wang YK, Perez-Jurado L, Paperna T, Cisco M, Francke U (2000) A physical map, including a BAC/PAC clone contig, of the Williams-Beuren syndrome: deletion region at 7q11.23. Am J Hum Genet 66:47–68

Petek E, Jenne DE, Smolle J, Binder B, Lasinger W, Windpassinger C, Wagner K, Kroisel PM, Kehrer-Sawatzki H (2003) Mitotic recombination mediated by the *JJAZF1* (*KIAA0160*) gene causing somatic mosaicism and a new type of constitutional *NF1* microdeletion in two children of a mosaic female with only few manifestations. J Med Genet 40:520–525

Rasmussen SA, Colman SD, Ho VT, Abernathy CR, Arn PH, Weiss L, Schwartz C, Saul RA, Wallace MR (1998) Constitutional and mosaic large *NF1* gene deletions in neurofibromatosis type 1. J Med Genet 35:468–471

Reiter LT, Hastings PJ, Nelis E, De Jonghe P, Van Broeckhoven C, Lupski JR (1998) Human meiotic recombination products revealed by sequencing a hotspot for homologous strand exchange in multiple HNPP deletion patients. Am J Hum Genet 62:1023–1033

Reiter LT, Murakami T, Koeuth T, Pentao L, Muzny DM, Gibbs RA, Lupski JR (1996) A recombination hotspot responsible for two inherited peripheral neuropathies is located near a mariner transposon-like element. Nat Genet 12:288–297

Schmid P, Schulz WA, Hameister H (1989) Dynamic expression pattern of the *myc* protooncogene in midgestation mouse embryos. Science 243:226–229

Sengupta K, Rao BJ (2002) Translin binding to DNA: recruitment through DNA ends and consequent conformational transitions. Biochemistry 41:15315–15326

Shaikh TH, Kurahashi H, Saitta SC, O'Hare AM, Hu P, Roe BA, Driscoll DA, McDonald-McGinn DM, Zackai EH, Budarf ML, Emanuel BS (2000) Chromosome 22-specific low copy repeats and the 22q11.2 deletion syndrome: genomic organization and deletion endpoint analysis. Hum Mol Genet 9:489–501

Shaw CJ, Lupski JR (2004) Implications of human genome architecture for rearrangement-based disorders: the genomic basis of disease. Hum Mol Genet 13:R57–R64

Stankiewicz P, Lupski JR (2002) Genome architecture, rearrangements and genomic disorders. Trends Genet 18:74–82

Tonsgard JH, Yelavarthi KK, Cushner S, Short MP, Lindgren V (1997) Do *NF1* gene deletions result in a characteristic phenotype? Am J Med Genet 73:80–86

Valero MC, de Luis O, Cruces J, Perez Jurado LA (2000) Fine-scale comparative mapping of the human 7q11.23 region and the orthologous region on mouse chromosome 5G: the low-copy repeats that flank the Williams-Beuren syndrome deletion arose at breakpoint sites of an evolutionary inversion(s). Genomics 69:1–13

Wu BL, Austin MA, Schneider GH, Boles RG, Korf BR (1995) Deletion of the entire *NF1* gene detected by the FISH: four deletion patients associated with severe manifestations. Am J Med Genet 59:528–535

Wu BL, Schneider GH, Korf BR (1997) Deletion of the entire *NF1* gene causing distinct manifestations in a family. Am J Med Genet 69:98–101